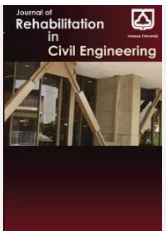

Journal of Rehabilitation in Civil Engineering

Journal homepage: https://civiljournal.semnan.ac.ir/

Effect of Molarity of Sodium Hydroxide on the Strength Behavior of Fiber-Reinforced Geopolymer Concrete Exposed to Elevated Temperature

Abbasali Saffar [1]; Mohammad Ehsanifar [2,*]; Seyed Mohammad Mirhosseini [3]; Mohammad Javad Taheri Amiri [4]

1. Ph.D. Student, Department of Civil Engineering, Arak Branch, Islamic Azad University, Arak, Iran
2. Associate Professor, Department of Industrial Engineering, Arak Branch, Islamic Azad University, Arak, Iran
3. Assistant Professor, Department of Civil Engineering, Arak Branch, Islamic Azad University, Arak, Iran
4. Assistant Professor, Department of Civil Engineering, higher education institute of Pardisan, Freidonkenar, Iran

* Corresponding author: *m-ehsanifar@iau-arak.ac.ir*

ARTICLE INFO

Article history:
Received: 29 March 2023
Revised: 22 June 2023
Accepted: 05 July 2023

Keywords:
Strength behavior;
Ternary blended GPC;
Molarity;
Elevated temperature;
Artificial intelligence.

ABSTRACT

Ordinary concrete production is highly energy intensive and caused to greenhouse gas emission responsible for global warming. Geopolymer mixtures are the eco-friendly alternative for to protect the CO_2 emission in concrete industry. In this study, the post-fire behavior of fiber reinforced geopolymer concrete (FRGPC) was investigated based on molarity changing approach. To do so, supplementary cementitious materials such as fly ash, metakaolin and zeolite are used to provide binary and ternary FRGPC mixtures. For this aim, FRGPC exposed to elevated temperature at the 200, 500, 800 °C. In addition, three molarity (12, 14, 16) of solution is studied for better strength performance. The result of this study presented that the ratio of the post-fire residual strength of the sample of Z10MK20 increased by 8.1% at 200 °C, 14.1% at 500 °C, and decreased by 5.2% at 800 °C. The 28-day sample resistance, with 20% replacement of metakaolin, was measured at 45.8 MPa after adding fibers (2% constant volume of 1-3% polypropylene fibers). Also, with increasing the molarity of FRGPC mixtures from 12 to 16, the heat resistance behavior in FRGPC had an increase about 6%. Increasing the volume of polypropylene (PP) fibers up to 3% by volume did not have much effect on the heat resistance behavior of FRGPC. Beside, post-fire strength of FRGPC was predicted using artificial neural network (ANN) and support vector machines (SVM) with the integration of water cycle algorithm (WCA). Based on the coefficient of determination obtained in the training and testing stages, ANN-WCA model had an acceptable performance in predicting the post-fire residual strength of FRGPC. Additionally, the sensitivity analysis manifested that the molarity of the FRGPC mixtures and the exposed temperature had the greatest effect and PP fibers had the least effect on post-fire residual strength of FRGPC.

E-ISSN: 2345-4423

How to cite this article:
Saffar, A., Ehsanifar, M., Mirhoseini, S. M., & Taheri Amiri, M. J. (2024). Effect of Molarity of Sodium Hydroxide on the Strength Behavior of Fiber-Reinforced Geopolymer Concrete Exposed to Elevated Temperature. Journal of Rehabilitation in Civil Engineering, 12(2), 111-128. https://doi.org/10.22075/jrce.2023.30282.1831

1. Introduction

Concrete is a commonly utilized material worldwide due to the widespread availability of ordinary Portland cement (OPC), which serves as the primary binder with simple preparation and exceptional mechanical characteristics[1]. However, the escalating need for concrete leads to amplified energy consumption and carbon dioxide emissions in the production of a significant quantity of OPC [2]. The excessive use of OPC is considered one of the primary drivers of global warming, and, therefore, several endeavors have been undertaken to identify eco-friendly alternatives to this material[3]. Geopolymer prepared to replace OPC by activating aluminosilicate supplementary cementitous materials (SCMs) with high alkali solution [4]. Geopolymer concrete (GPC) can be generated from a variety of sources, including industrial waste and geological materials such as fly ash (FA), metakaolin (MK), zeolite (ZE), among others [5].

Geopolymer composites based on fly ash (FA) have received extensive attention in the academic research community, owing to the fact that thermal power generation is responsible for the emission of a significant quantity of FA. [6]. Furthermore, the notable abundance of essential raw materials and favorable activity have rendered MK a subject of significant interest [7,8]. The incorporation of ZE in the Fly Ash-based GPC enhances the degree of geopolymerization, attributed to the micro-aggregate phenomenon of the finely divided zeolite particles. [9].

In the recent years, there has been a considerable amount of research undertaken by analysts exploring the potential utilization of various industrial byproducts and wastes such as waste glass powder, metakaolin, phosphate sludge, rice husk ash, fly ash, etc. as a primary raw material or as fine or coarse aggregates in the production of GPC [10]. The mechanical properties of GPC are subject to the influence of various industrial byproducts and wastes. Deb et al. [11] conducted an investigation whereby they utilized industrial blast furnace waste slag as a partial substitute for fly ash in the preparation of GPC. They observed notable enhancements in both tensile and compressive strengths upon the integration of slag. Similarly, Okoye et al. [12] found that the use of micro-silica to replace fly ash in GPC resulted in enhanced strength properties. Luhar et al. [13] employed rubber tire waste in fibrous form to partially substitute fine aggregates in the production of geopolymer fly ash concrete, and noted that while an increase in the percentage of the waste led to a decrease in compressive strength, there was an increase in both flexural and tensile strength. Park et al. [14] also observed a decrease in compressive strength when sand was replaced with crumb rubber in GPC that had fly ash as the base material.

A systematic reduction in strength was observed by Aly et al. [15] through their investigation. This phenomenon was observed as the crumb rubber content was gradually increased to serve as a substitute for natural sand and aggregates in the structure of geopolymer concrete. Albitar et al. [16] utilized granulated lead smelter slag as a sand replacement in geopolymer concrete and observed that the compressive strength gradually decreased with the increasing amount of slag. Muttashar et al. [17] investigated the use of fine garnets to replace sand in GGBS-based self-consolidating GPC and concluded that an increase in the amount of garnets had a negative impact on the mechanical properties.

Although the early strength of the geopolymer containing low calcium FA being less than that of the MK-based geopolymer, the MK-based geopolymer displays inferior resistance to high temperature when compared to FA-based geopolymer [18]. To address these limitations, some scholars have developed binary and

ternary blended geopolymer concrete (GPC) by incorporating a combination of fly ash (FA), metakaolin (MK), and ground granulated blast-furnace slag (GGBFS). The research findings indicate that geopolymer composed of FA-MK-GGBFS displays superior compressive and bending strengths and enhanced high-temperature endurance when compared to geopolymer concrete made with either MK or FA [19].

The sodium hydroxide (NaOH) is the only activator in the GPC that provides excellent mechanical properties compared to the OPC concrete [10]. The incorporation of sodium silicate, also known as Na_2SiO_3, into the mixture resulted in a notable improvement in the early strength, specifically during the 7-28 day period, of the geopolymer system. [12]. The addition of a higher concentration of NaOH in the mixture has been observed to improve the concrete's strength, although it comes at the expense of reduced workability of the fresh mix. [18]. The GGBFS content in the GPC mix forms the calcium silicate hydrate (C-S-H) bond if the NaOH concentration is low or less alkalinity [20].

Of the above factors, incorporating fibers into concrete can improve its strength and toughness, as evidenced by numerous studies that have investigated various types of fibers, including synthetic, natural, and metal. Many studies have examined various types of fibers, including metal, synthetic, and natural. Adding fibers can increase tensile strength and decrease crack length in concrete. Consequently, fiber-reinforced concrete is more ductile and durable than non-fiber concrete [21,22]. Due to its good mechanical properties and environmental protection qualities, GPC is being considered as a replacement for silicate cement concrete. To evaluate its performance, various studies have examined fiber-reinforced GPC, with carbon, steel, glass, polyvinyl alcohol, polypropylene (PP), cotton, and natural fibers being used as reinforcement [23–26]. Moreover, in this study, machine learning (ML) approach was implemented to modeling the GPC characteristics. ML is well known approach in data science because of its capability to create predictive data-intelligence models [27–31].

According to the literature, it can be seen that researchers have not comprehensive investigation on utilizing ternary blended pozzolanic materials in fiber reinforced GPC under elevated temperature. Beside experimental investigation, compressive strength and post-fire strength of ternary blended fiber reinforced GPC is simulated using artificial intelligence models in order to formulate the target variable (i.e., post-fire strength). Consequent, the most important variables are prioritized using sensitivity analysis.

2. Materials and methods

2.1. Materials specifications

a)SCMs

In this research, the low calcium FA with a granule density of 2.66 g/cm^3 was maintained from Foolad Mobarakeh Co. in Esfahan. In addition, the used Clinoptilolite type of ZE for this study was supplied from Semnan mines in Iran, and had a specific gravity of 2.14 and Blaine fineness of 6788 cm^2/g. Moreover, Delijan MK was used as pozzolan which was supplied from the Ferro Alloy Industries Co. having a granule density of 2.59 g/cm^3. The total amount of aluminum Oxide (Al_2O_3), SiO_2, and Iron(III) oxide (Fe_2O_3) in the ZE was about 80%. This value is higher than the lowest required amount (70%) that is suggested by ASTM C 618 [32] for natural pozzolans. The chemical properties and loss on ignition (LOI) of the used pozzolans are given in Table 1. In the mentioned table due to the rounding of the values, the sum of the percentages of different components is not equal to 100%.

Table 1. Chemical composition of utilized materials. (%).

Component (%)	ZE	FA	MK
SiO_2	67.79	61.3	52.1
Al_2O_3	13.66	28.8	44.7
Fe_2O_3	1.44	4.98	0.8
CaO	1.68	1.05	0.09
MgO	1.2	0.63	0.03
SO_3	0.5	0.13	-
Na_2O	2.04	0.24	9.1
K_2O	1.42	1.4	0.03
Loss of ignition	10.23	0.7	0.7
Specific gravity	2.3	2.6	2.6
Fineness (m^2/kg)	320	310[a]	12000

a) Alkaline solution

The alkaline solution used in the presented study to activate the SCM (e, g., FA, MK and ZE) was a compound of glass water and sodium hydroxide. The solid sodium hydroxide 96% was prepared as a water-soluble solution. The sodium silicate solution utilized in this research had a SiO_2 / Na_2O ratio equal to 2.27 (SiO_2 = 35.9%, Na_2O = 15.8 %,).

a)Fibers

The experimental investigation for development of eco-friendly and structural GPC mixtures were performed using 2-part hybrid fibers namely steel (ST) and PP. Table 2 referred the details of used fibers. The PP fiber length of 6 mm was utilized to reinforce the GPC. Moreover, in this study, the hooked-end steel fibers having a maximum length equal to 5mm and a diameter equal to 0.12 mm were used to develop and propose the optimal blends. To do so, PP at 0.75, 1, 1.25 vol% and St at 2 vol%, were added in GPC mixture proportions.

Table 2. Fiber properties.

	PP	**ST**
Length (mm)	6	5
Density (gr/cm^3)	0.93	7.8
Tensile strength (MPa)	400	2500
Water absorbency	No	No
Alkaline and acid resistant	Excellent	Excellent
Diameter (mm)	-	0.12

a) Aggregates

Fine aggregate (Fa) and coarse aggregate (Ca) constituted about 77% of the concrete volume. The natural sand used as fine aggregate was prepared from a local quarry having a fineness modulus equal to 3.05, which was in the recommended range by ASTM C33 [33]. The used recycled coarse aggregate had a maximum grain size of 12.5 mm. Also, the specific gravity and water absorption values were equal to 2.57 and 1.52%, respectively. Figure 1 demonstrates the sieve analyses corresponding to the recycled and fine coarse aggregates.

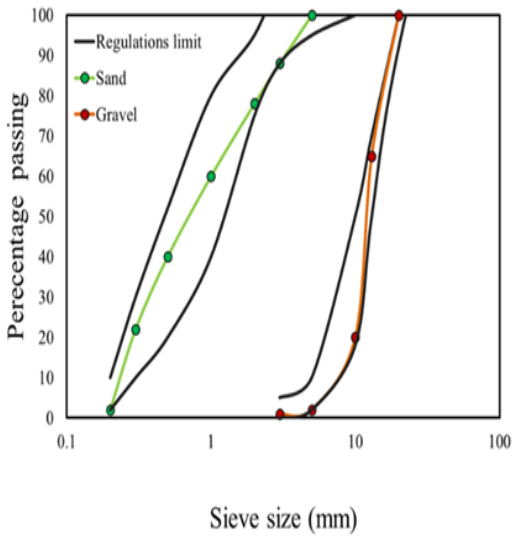

Fig. 1. Gradation curve for the used.

2.2. Mix design, specimen preparation and testing procedure

The mixing of the GPC mixtures was conducted in a mixer. For this aim, dry materials such as Fa and Ca and SCMs were mixed for approximately 3 minutes in the mixer, next the alkaline solution was added to the mixture and the wet mixing continued for another 4–6 minutes until a consistent mixture was prepared. The fresh mixtures were dumped into steel cube molds with 150×150×150 mm and cylindrical specimens with 150×300 mm. The molds were filled in two layers and each layer was vibrated for about 25 second using a vibrating table. Table 3 presents the mix design of reinforced GPC mixtures.

Table 3. Mix design of GPC specimens.

Specimen	SCM			Fa (Kg/m^3)	Ca (Kg/m^3)	PP (%)	Na_2Sio_3 (Kg/m^3)	NaOH (Kg/m^3)
	FA (Kg/m^3)	ZE (w%)	MK (w%)					
GR0	500	0	0	500	1036	0	162	108
MK10	450	0	10	500	1036	0	162	108
MK20	400	0	20	500	1036	0	162	108
Z10-MK10	400	10	10	500	1036	0	162	108
Z10-MK20	350	10	20	500	1036	0	162	108
Z20-MK10	350	20	10	500	1036	0	162	108
Z20-MK20	300	20	20	500	1036	0	162	108
GR0-PP1	500	0	0	500	1036	1	162	108
MK10-PP1	450	0	10	500	1036	1	162	108
MK20-PP1	400	0	20	500	1036	1	162	108
Z10-MK10-PP1	400	10	10	500	1036	1	162	108
Z10-MK20-PP1	350	10	20	500	1036	1	162	108
Z20-MK10-PP1	350	20	10	500	1036	1	162	108
Z20-MK20-PP1	300	20	20	500	1036	1	162	108
GR0-PP2	500	0	0	500	1036	2	162	108
MK10-PP2	450	0	10	500	1036	2	162	108
MK20-PP2	400	0	20	500	1036	2	162	108
Z10-MK10-PP2	400	10	10	500	1036	2	162	108
Z10-MK20-PP2	350	10	20	500	1036	2	162	108
Z20-MK10-PP2	350	20	10	500	1036	2	162	108
Z20-MK20-PP2	300	20	20	500	1036	2	162	108
GR0-PP3	500	0	0	500	1036	3	162	108
MK10-PP3	450	0	10	500	1036	3	162	108
MK20-PP3	400	0	20	500	1036	3	162	108
Z10-MK10-PP3	400	10	10	500	1036	3	162	108
Z10-MK20-PP3	350	10	20	500	1036	3	162	108
Z20-MK10-PP3	350	20	10	500	1036	3	162	108
Z20-MK20-PP3	300	20	20	500	1036	3	162	108

2.3. Compressive strength test

The compressive strength test referred to as the most prevalent evaluation conducted on concrete in construction is widely recognized for providing a comprehensive overview of all the characteristics of concrete. On the basis of this assessment, the concrete work can be either accepted or declined. The compressive strength, regarded as a concrete property, is influenced by numerous factors linked to the quality of the materials employed, the mix design, and the quality control throughout the concrete production process. Depending on the code implemented, the test sample may be a cylinder with diameter 15 cm and height of 30 cm or a cube of size 15 × 15 × 15 cm.

As outlined by ASTM C39 [33], a standardized method exists to obtain the compressive strength of concrete. This entails the careful pouring of concrete into a mold, with adequate compaction to minimize void volume. Subsequently, the molds are removed and the resulting test specimens undergo water curing for a period of 3, 7, 28, 56, or 91 days, as specified. At the end of this curing period, the specimens are subjected to compression testing using a machine, with an incremental application of load until failure occurs.

2.4. Artificial neural network (ANN)

Artificial neural networks (ANNs) are a form of parallel processing that consist of a large number of processing elements or neurons interconnecting through layers and weights, alike the structure of biological nervous systems [34,35]. The calibration process involves a comparison between the model's target variables and the measured outputs, followed by the back-propagation of errors to modify the initially assigned weights. consequently, the final weights are calculated via error minimization [36].

The input x variable is evaluated through the application of a weighted summation of the outputs generated by the first layer. This resultant value is then allotted to each respective neuron within the second and third layers. As an example, the computation of the value for y within the jth neuron of the second layer is determined by the ensuing algorithm:

$$y_{pj} = \sum_{i=1}^{I} W_{ij} O_{pi} + \theta_j \quad (1)$$

where θ_j, O_{pi} and W_{ij} represent the bias for neuron j, the ith output of the first layer and the weights between first and second layers, respectively. A nonlinear activation function is employed on the dependent variable, y, and subsequently, the resulting output, denoted as $f(y)$, is computed for each neuron located in the second and third layers [37]. Eq. 2 is defined to calculate logistic function as a most common activation function:

$$f(y) = \frac{1}{1+e^{-y}} \quad (2)$$

2.5. Support vector machine (SVM)

Derived from Support Vector Machines, a prevalent machine learning approach utilized in the fields of soft computing and concrete technology, this precise method is proficient in resolving nonlinear classification, regression, and function prediction tasks.[38,39]. In contrast to the traditional support vector machine (SVM) approach, which involves solving a convex quadratic programming problem, the SVM solution is arrived at through the utilization of the least squares method to solve a linear equation system. [40]. The SVR function can be derived from the provided input and output variables in the following manner:

$$y = w^T \varphi\,(X) + b \quad (3)$$

where w is the m-dimensional weight vector, φ is the mapping function and b is the bias term. Cortes and Vapnik [41] proposed the integration of an additional slack variable in the linear SVR classifier to allow for generalization of the classification model to include non-separable data instances. The introduction of this auxiliary variable brings

about notable modifications to the existing system of inequalities.

$$q_k[w^T p_k + b] \geq 1 - \xi_k \qquad k = 1,2,3,\dots,N \quad (4)$$

Now, the issue at hand has been greatly simplified in the SVR framework. The resolution now entails solving a mere set of linear equations, in contrast to a convex quadric program. [42]. In the primal space, the SVM classification method is expressed as follows:

$$q(p) = sign[w^T p + b] \quad (5)$$

$$C(B) = (B + 1) + dB \quad (6)$$

2.6. Water cycle algorithm (WCA)

The concept of WCA is derived from the careful observation of natural phenomena, particularly the movement of rivers and streams towards the sea. The majority of these water bodies originate from elevated mountainous regions, where the melting of snow and glaciers initiates their flow towards lower elevations. During this journey, they accumulate additional water from rainfall and other streams before ultimately draining into the sea. The hydrologic cycle, which governs the movement of water, involves the evaporation of water from lakes and rivers, as well as transpiration by plants and trees during photosynthesis. This water is then transferred to the atmosphere, where it gives rise to the formation of clouds. When the atmospheric temperature decreases, these clouds condense and precipitate back to the earth in the form of rain or snow [43]. Underground water resources and aquifers are replenished through the processes of snow melting and rainfall. The subterranean water flows beneath the terrain with a similar dynamic to that of surface water flow. Moreover, the water present in rivers and streams undergoes an evaporation process, thus perpetuating the cycle [44].

At the onset of the proposed method, a raindrop is designated as the initial population, in accordance with established practice for other metaheuristic algorithms. The presence of precipitation is presupposed in the first instance. Subsequently, the most exemplary raindrop (or individual) is identified as the sea, while a multitude of commendable raindrops are deemed the river. In a N_{var} dimensional optimization program, a raindrop is an array of $1\times N_{var}$. This array is expressed as following function:

$$Raindrop = [x_1, x_2, x_3, \dots . x_N] \quad (7)$$

2.7. Performance metrics

In this study, to evaluate the proposed models, several performance measures (Eqs. (8)- (10)) were used. The correlation coefficient (R), root mean square error (RMSE), mean absolute error (MAE), were used as the measure of precision which are expressed as following:

$$R = \frac{\sum_{i=1}^{M}(O_i - \overline{O}).(P_i - \overline{P})}{\sqrt{\sum_{i=1}^{M}(O_i - \overline{O})^2 \sum_{i=1}^{M}(P_i - \overline{P})^2}} \quad R \geq 0.8 \quad (8)$$

$$RMSE = \frac{\sum_{i=1}^{M}(P_i - O_i)^2}{M} \quad RMSE = (0, +\infty) \quad (9)$$

$$MAE = \frac{\sum_{i=1}^{M}|P_i - O_i|}{M} \quad RMSE = (0, +\infty) \quad (10)$$

3. Analysis of experiments and review of results

3.1. The results of the effect of molarity on compressive strength

Using the samples made at the age of 28 days in a thermal furnace at temperatures of 200, 500, and 700 °C for the investigation of ternary blended GPC's resistance behavior under heat, Figure 2 shows how the samples were tested for stability and sample authority. Figures 3-5 shows the results of a study that looked at the effect of molarity on compressive strength under the heat of a ternary blended geopolymer based on metakaolin, zeolite and fly ash. At 20 degrees' Celsius laboratory temperature, the 28-day compressive strength under the heat of mixtures containing

metakaolin, including MK20 and Z10-M20 with 12 molarity, was 45.8 MPa and 45.4 MPa, respectively. In the design and construction of geopolymer mixtures, by reducing the amount of fly ash and increasing metakaolin and zeolite, the results of resistance behavior have grown significantly. By applying heat in a thermal furnace up to 500 °C, the trend of thermal resistance is increasing, and from this temperature, the resistance of the samples decreased by applying higher heat.

Fig. 2. Fiber reinforced GPC specimens and exposing to the heat temperature.

The compressive strength increased at both laboratory and elevated temperatures by increasing the molarity of the alkaline solution from 12 to 14, while it decreased at 16 molarity. To produce geopolymeric gel, alkaline activating solutions, particularly sodium hydroxide, dissolve Si and Al in aluminosilicate sources and produce SiO_4 and AlO_4.

When an alkaline activator solution is mixed with sodium silicate, the amount of SiO_4 and the rate of the geopolymerization reaction increase, thus resulting in an increase in the compression strength of geopolymer concrete to a certain extent due to the presence of soluble Si. Additionally, if less sodium silicate solution is added than is optimal, the amount of dissolved Si decreases, reducing the amount of SiO_4, thereby decreasing the compressive strength.

3.2. The results of the effect of PP fiber on compressive strength

Figure 4 shows the results of a 28-day compressive strength test on ternary blended fiber reinforced GPC (FRGPC). In samples without fibers containing 10% substituted metakaolin, the 28-day compressive strength was 26.64 and 37.5 MPa. 28-day concrete samples increased by 3% when 0.5% of polypropylene fibers were added.

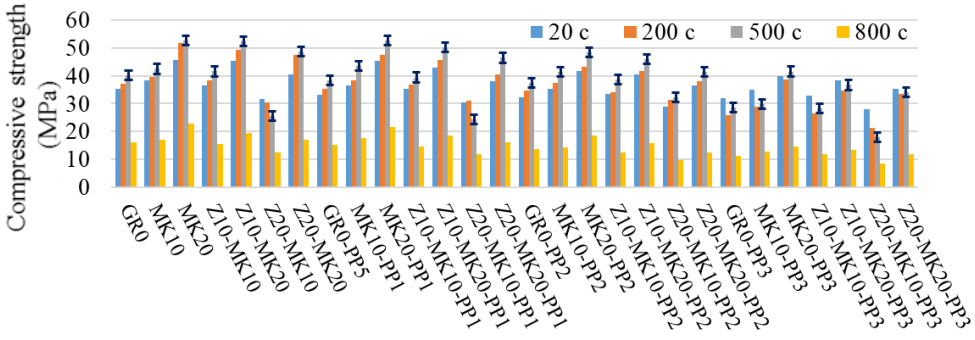

Fig 3. Compressive strength results of the reinforced fiber GPC with 12 molarity content.

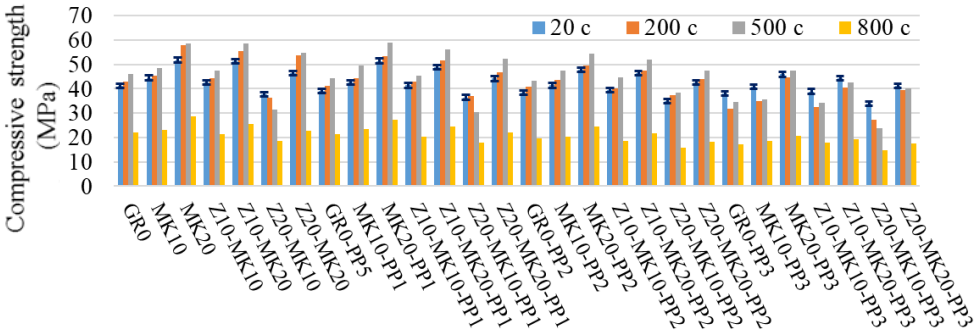

Fig. 4. Compressive strength results of the reinforced fiber GPC with 14 molarity content.

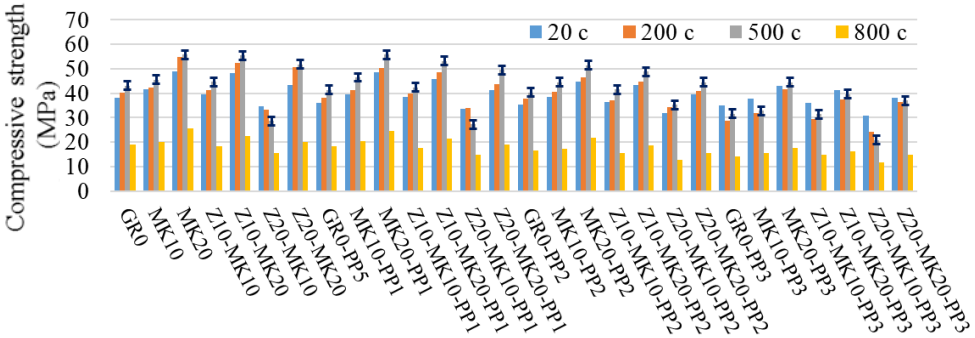

Fig. 5. Compressive strength results of the reinforced fiber GPC with 16 molarity content.

When the amount of fibers was increased to 1%, the compressive strength of geopolymer concrete at 28 days decreased by 43.6, and when the amount of fibers was increased further, the compressive strength of the concrete was further decreased. The process was repeated for 20% and 30% substitutions of metakaolin base material, increasing compressive strength by adding 0.5% polypropylene fibers and decreasing it by adding 1% and 1.5% volume percent of fibers, respectively. Using 0.3% polypropylene fibers increased compressive strength by 6%, according to Asrani et al [35]. Their results showed that as the fiber amount increased, the compressive strength decreased, which may be associated with the contact zone. It can be concluded from the obtained results that PP fibers have a negative impact on FRGPC compressive strength, and only at the optimal percentage do they increase it by approximately 5%. The addition of PP fibers up to 0.5% may increase compressive strength due to increased bonding forces between the components of the FRGPC mixtures. Figure 6 shows that the compressive strength decreases as the fiber percentage increases at 800 degrees Celsius. When fibers are increased, the decreasing slope between 200 and 500 degrees Celsius shows a greater value.

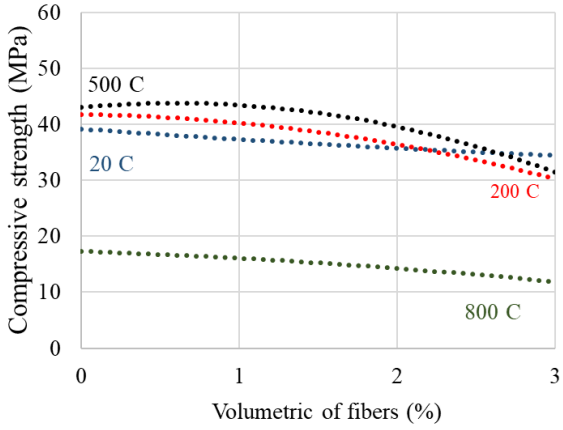

Fig. 6. Compressive strength of GPC with regard to the percentage of PP under elevated temperature (12 molarity mix designs).

This contact zone, which is sometimes called the border layer or transition zone, is the

boundary between the cement paste or base material and the aggregate, fiber, or bar surface and plays a significant role in the durability, permeability, and strength of concrete. Contact zones have a different microstructure and more porosity than cement paste. The type of fiber, type of cement, type of pozzolan used, etc., determine the thickness of the contact zone. The fibers used in this article are polymer fibers, and, due to their high flexibility, tend to pelletize and create holes in the matrix of base material when used in a high-volume percent. This results in internal defects in the contact zone, leading to a reduction in the compressive strength of geopolymer concrete. Furthermore, in conclusion, adding fibers to geopolymer concrete did not significantly increase its compressive strength. Figure 7 shows the failure of the 28-day geopolymer concrete sample without the presence of steel fibers and PP.

Fig. 7. The Z10-MK20-PP2 specimen.

3.3. Simulating the compressive strength of geopolymer concrete

After making geopolymer concrete samples and performing mechanical tests, the results were collected in an Excel file. Forecasts usually choose independent variables that are easy to measure and cost little to measure. In addition, the prediction results depend on the parameters selected, and the predicted accuracy is used to evaluate the correctness of the prediction. The first stage of this research was to determine whether the selected variables (model input) can easily be determined by laboratory experiments and, second, that the results are accessible at the lowest cost. Based on the results of the laboratory tests, the database contains 336 data from 28 geopolymer three-component mix designs with molarities 12, 14, and 16, which were prepared at temperatures of 20, 200, 500, and 700 degrees Celsius in order to evaluate resistance behavior. During modeling, coarse grain (C), fine grain (F), and the volume percentage of steel fibers in geopolymer concrete, which are fixed characteristics in the mix design, were not considered. The model input variables are fly ash (FA), zeolite (ZE), metakaolin (MK), total fiber volume (V_f), molarity (M), and temperature (T), and the model output parameter is concrete compressive strength (CS). In order to prevent overfitting, the data set was divided into two groups; training and testing. This technique uses 75% of the data for training, and 25% of the data for evaluating the network built during training. The fundamental difference between the training data and the testing data lies in the fact that the former constitutes a subset of the original data that is utilized to train the model of artificial intelligence, while the latter is utilized to verify the precision of the model. Typically, the training dataset is more larger as compared to the testing dataset.

3.3.1. Development of ANN model to predict compressive strength under the heat of multi-component fibrous geopolymer concrete

In this research, a perceptron multi-layer neural network is used, which has a hidden layer. In the pursuit of identifying the ideal quantity of neurons situated within the hidden layers, a total of twenty neural network models were generated and thoroughly assessed. This was accomplished by increasing the number of nerves in the first hidden layer one by one (1-

20) and checking their performance. The Levenberg-Marquardt algorithm was used to train the neural network. The backpropagation algorithm is widely acknowledged for its swiftness and frequently suggested as the foremost choice for supervised training. A sigmoidal and linear logarithm function was used to determine the optimal stimulation function in the hidden layer as well as the output in the sigmoidal tangent. The sigmoidal tangent function in the hidden layer and the linear function in the output layer gave the best result. For training and testing networks, 25% (83 data) and 75% (253 data) of the information have been used. In the test phase, the final model is determined by its performance. Every time the artificial neural network model is analyzed in MATLAB software, different weights are assigned. Consequently, each analysis produces a different answer. An ANN model with 7 neurons in the hidden layer, 0.1 training rate, 0.1 momentum, and 1000 training rounds was recognized as the best neural network model in this study. The training rate was 0.01-0.9, the momentum index was 0.01-0.9, and the number of model repetitions was 1000-5000. The diagram in Figure 8 shows the evaluation criteria for each artificial neural network model. During the teaching and learning process, the repetition loop (Epoch) is stopped after 1000 rounds and the error is below 0.05. During this process, the Mean Square Error (MSE) will be calculated as follows:

$$MSE = \frac{1}{N}\sum_{i=1}^{N}(CS_{Pr} - CS_{es})^2 \quad (5)$$

3.3.2. Development of SVM model to predict compressive strength under the heat of multi-component fibrous geopolymer concrete

Based on the theory of optimization, support vector machines (SVM) are modeled with linear functions with high dimensions, and their learning algorithm is based on the theory of optimization. SVMs and radial basis function kernels were used in this study. As part of SVM modeling, the user sets parameters, such as the kernel type setting parameter (C), as well as kernel specific parameters and (GAMA), and (EPSILON). The choice of C and Epsilon was made by the user based on trial and error. Consequently, 25 SVM models were created based on the changes in the parameters, and finally, the SVM model with the following specifications was selected as the best (Table 4).

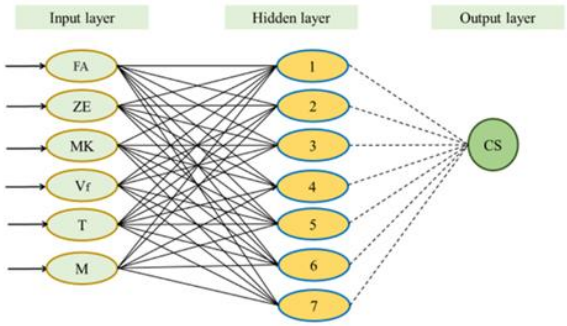

Fig. 8. schematic framework of ANN.

Table 4. hyper parameter values of SVM.

C	EPSILON	GAMA
0.15	232.2	**3.72**

3.3.3. Development of an optimized model of artificial neural network and support vector machines and water cycle algorithm to predict geopolymer concrete compressive strength

Coding for this method was done using MATLAB software. Artificial neural network training and support vector machines are both critically affected by weights and bias, despite constant architectures and other parameters. A method of trial and error was used to determine an optimal architecture in this study. MATLAB was used to write the program that performed trial-and-error automatically in order to select the best network architecture. Based on Root Mean Square Error (RMSE), this program finds the best architecture for a diverse number of neurons and hidden layers. As described in the previous section, this

architecture also uses the learning functions and algorithms of the ANN method. In the end, the WCA algorithm was used to optimize weights, and network bias. The best network architecture consists of six neurons in the hidden layer, eight neurons in the input layer, and one neuron in the output layer, according to the evaluations. According to Table 5 of the WCA algorithm, the number of repetitions per time and the numbers of particles are 100 and 50 respectively for optimizing the weight and bias of the network. As shown in Figure 9, artificial neural networks are used in the training phase to predict the compressive strength of geopolymer concrete. Additionally, this figure displays relative error values for the predictions made by the methods studied. Based on the value coefficient of 0.990, the optimized artificial neural network method with the water cycle algorithm predicted the compressive strength of the geopolymer concrete well.

Table 5. Values of parameters for WCA.

Parameter	Value
Hyper parameters	3
Population number	30
Lower bound	1
Upper bound	4
NSR	4
D_{MAX}	16^{-10}

At this stage, the highest average error was 1.281, which is analytically small and ignored. According to Figure 10, geopolymer concrete compressive strength values at the test stage are predicted based on laboratory compressive strength values. From a simulation perspective, the ANN-WCA model's performance with a drop in percentage has been acceptable. For this stage, the determination coefficient in the simulation of geopolymer concrete compressive strength was approximately 0.988, with a mean error of 1.269 MPa.

In Figure 11, the linear diagram shows the comparison between the computational compressive strength data and the observational data. Figure 9 shows how the ANN-WCA model, in the test stage, with considerable precision predicted the compressive strength of geopolymer concrete under heat, compared to other proposed methods. With the innovative water cycle algorithm integrated, the models displayed lower production errors and higher convergence rates. In this research, the WCA is evaluated as a stochastic search algorithm, which exhibits high convergence and simplicity, while also boasting low-cost and flexible computational performance [43] which is firstly utilized for tuning of ANN and SVM control parameters herein. The WCA algorithm enhances the average fitness of solutions, which present that this algorithm is able to effectively enhance the initial random population.

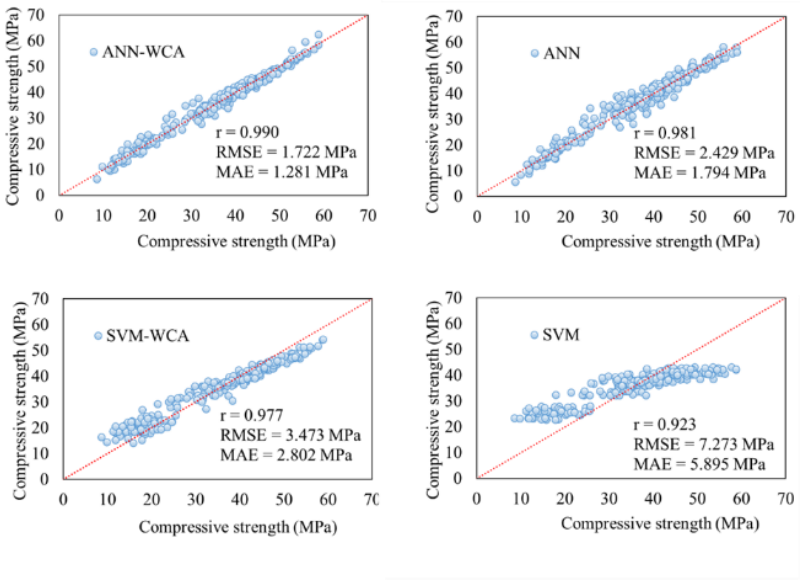

Fig. 9. Observed compressive strength vs. predicted values using ANN, SVM, ANN-WCA, and SVM-WCA models for training stage.

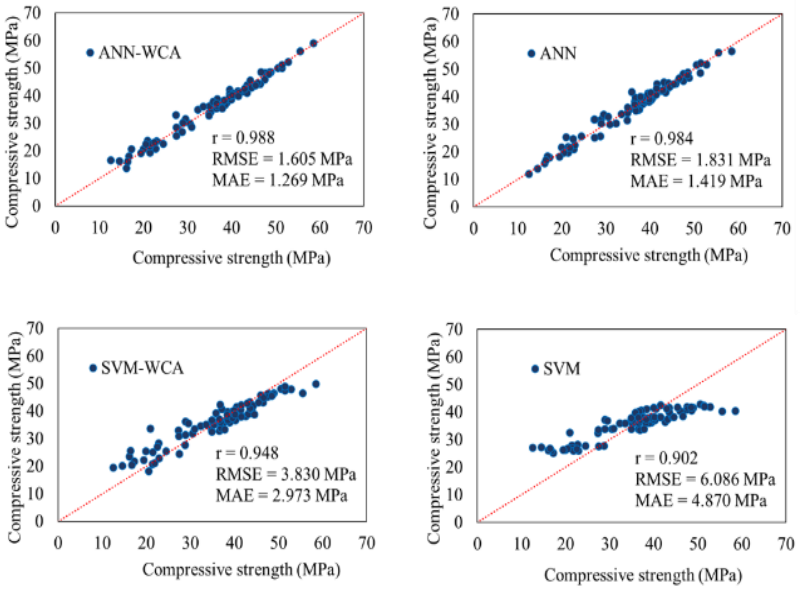

Fig. 10. Observed compressive strength vs. predicted values using ANN, SVM, ANN-WCA, and SVM-WCA models for testing stage.

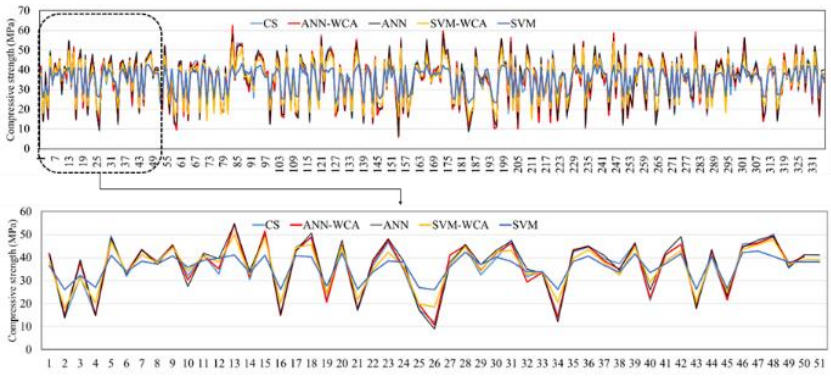

Fig. 11. The ANN-WCA predictions for compressive strength of reinforced GPC.

Sensitivity analysis is the analysis of the impact of dependent variables on independent variables, and their impact on each other. This study used an optimized artificial neural network model with a water cycle algorithm to perform a sensitivity analysis of each input parameter on the compressive strength of a three-component geopolymer concrete. For this purpose, an input parameter is removed and its effect on the output of the model is analyzed. According to the results of the sensitivity analysis, removing molarity input variables (R=0.71) and temperature (R=0.65) had the greatest impact on the developed model in predicting geopolymer concrete compressive strength. Also, the volume of fibers (R=0.84) has the lowest impact on the model output. Table 6 shows the full description of the sensitivity analysis of the parameters.

Table 6. Sensitivity analysis results.

Input parameters	R
$\mathrm{CS} = f\ (ZE, MK, Vf, T, M)$	0.8
$\mathrm{CS} = f\ (FA, MK, Vf, T, M)$	0.78
$\mathrm{CS} = f\ (FA, ZE, Vf, T, M)$	0.74
$\mathrm{CS} = f\ (FA, ZE, MK, T, M)$	0.84
$\mathrm{CS} = f\ (FA, ZE, MK, Vf, M)$	0.65
$\mathrm{CS} = f\ (FA, ZE, MK, Vf, T)$	0.71

4. Conclusion

The resistive and thermal behavior of a fiber reinforced geopolymer concrete (FRGPC) containing fly ash, zeolite, and metakaolin pozzolans was investigated in this study. Mixes were made and analyzed by examining how molarity influences geopolymer concrete behavior and fiber consumption.

- In the presence of molarity 12, under heat up to 500 °C, the residual post-fire strength increased, and heat, as a concrete microstructure generator, led to better setting and greater resistance. Compressive strength decreased significantly at 800 °C. The Z10MK20 sample's 28-day compressive strength is 45.4 MPa with 10% zeolite and 20% metakaolin as fly ash replacements. As a result of the 10% metakaolin replacement of fly ash, the compressive strength increased by 11.6% and 6.2%, respectively, for molarities 14 and 16.
- As a result of the obtained laboratory results, the ratio of the compressive strength of the sample of Z10MK20 increased by 8.1% at 200 °C, 14.1% at 500 °C, and decreased by 5.2% at 800 °C. The 28-day sample resistance, with 20% replacement of metakaolin, was measured at 45.8 MPa after adding fibers (2% constant volume of 1-3% polypropylene fibers).
- The compressive strength of FRGPC's 28-day was increased to 27.3 MPa with the addition of 1% polypropylene fibers. By increasing the amount of fibers to 2%, geopolymer concrete's compressive strength decreased for 28 days to 41.4 MPa.
- In this research, after achieving laboratory results and analysis, we developed an optimized innovative model that combined artificial neural network (ANN) methods and support vector machines (SVM) with water cycle optimization algorithm (WCA) to simulate the resistance behavior under the geopolymer multi-component mixed

heat. Simulated results indicate that the optimized ANN method in conjunction with the WCA is effective in predicting FRGPC residual post-fire strength based on the value coefficient of 0.990 based on performance metrics as presented in litteratutue [45,46],

- As a result of the experimental stage, the accuracy of the ANN-WCA and SVM-WCA model was acceptable in terms of modeling performance in the prediction of FRGPC's strength was approximately 0.988 and 0.948, respectively. In order to achieve maximum strength, the constituent materials in geopolymer concrete were prioritized based on sensitivity analysis.
- A sensitivity analysis of the developed model revealed that the removal of the molarity and temperature input variables had the highest impact on predicting the compressive strength under the heat of mixed multi-component fiber geopolymer with a coefficient of determination of 0.71 and 0.65, respectively.

Although, the geopolymer mixtures needs higher temperature curing but the more casting and curing parameters like moisture and pressure are important. Also efflorescence is also a critical challenge for GPC. Therefore, using the mineral and industrial by-product materials in micro and Nano-size could be improve curing challenges and enhance the mechanical behavior and post-fire strength. Moreover, to better understanding of the performance of GPC mixtures, microstructural test such as X-ray diffraction (XRD) analysis and scanning electron microscopy (SEM) were necessitated for investigate the performance of GPC mixtures.

Besides, the findings of this study identified the superiority of the ANN-WCA and SVM-WCA in constructing innovative and precise approaches. It was shown that the proposed evolutionary algorithm with the optimized ANN and SVM control parameters not only enhanced the accuracy but also increased the robustness and reliability of the modeling of the GPC compared to the standard ANN and SVM method. In a forthcoming investigation, it might be achievable to overcome the modeling restriction by combining efficient data mining methodologies like input feature selection and data pre-processing, with advanced global optimization algorithms which possess high convergence speed.

References

[1] Amran M, Huang SS, Debbarma S, Rashid RSM. Fire resistance of geopolymer concrete: A critical review. Constr Build Mater 2022;324:126722. https://doi.org/10.1016/J.CONBUILDMAT.2022.126722.

[2] Phoo-Ngernkham T, Sata V, Hanjitsuwan S, Ridtirud C, Hatanaka S, Chindaprasirt P. High calcium fly ash geopolymer mortar containing Portland cement for use as repair material. Constr Build Mater 2015;98:482–8. https://doi.org/10.1016/J.CONBUILDMAT.2015.08.139.

[3] Jumaa NH, Ali IM, Nasr MS, Falah MW. Strength and microstructural properties of binary and ternary blends in fly ash-based geopolymer concrete. Case Stud Constr Mater 2022;17:e01317. https://doi.org/10.1016/J.CSCM.2022.E01317.

[4] Prasad Burle V, Kiran T, Anand N, Andrushia D, Al-Jabri K. Post-fire investigation on the mechanical properties and physical characteristics of fibre-reinforced geopolymer concrete. J Struct Fire Eng 2023;ahead-of-print. https://doi.org/10.1108/JSFE-01-2023-0016/FULL/XML.

[5] Sasi Rekha M, Sumathy SR. Engineering properties of Self-cured Geopolymer concrete binded with supplementary cementitious materials. Mater Today Proc 2022;69:879–87. https://doi.org/10.1016/J.MATPR.2022.07.357.

[6] Huang Y, Han M, Yi R. Microstructure and properties of fly ash-based geopolymeric material with 5A zeolite as a filler. Constr Build Mater 2012;33:84–9. https://doi.org/10.1016/J.CONBUILDMAT.2012.01.014.

[7] Albidah A, Alqarni AS, Abbas H, Almusallam T, Al-Salloum Y. Behavior of Metakaolin-Based geopolymer concrete at ambient and elevated temperatures. Constr Build Mater 2022;317:125910. https://doi.org/10.1016/J.CONBUILDMAT.2021.125910.

[8] Moradikhou AB, Esparham A, Jamshidi Avanaki M. Physical & mechanical properties of fiber reinforced metakaolin-based geopolymer concrete. Constr Build Mater 2020;251:118965. https://doi.org/10.1016/J.CONBUILDMAT.2020.118965.

[9] Kaya M, Koksal F, Gencel O, Munir MJ, Kazmi SMS. Influence of micro Fe2O3 and MgO on the physical and mechanical properties of the zeolite and kaolin based geopolymer mortar. J Build Eng 2022;52:104443. https://doi.org/10.1016/J.JOBE.2022.104443.

[10] Gülşan ME, Alzeebaree R, Rasheed AA, Niş A, Kurtoğlu AE. Development of fly ash/slag based self-compacting geopolymer concrete using nano-silica and steel fiber. Constr Build Mater 2019;211:271–83. https://doi.org/10.1016/J.CONBUILDMAT.2019.03.228.

[11] Deb PS, Nath P, Sarker PK. The effects of ground granulated blast-furnace slag blending with fly ash and activator content on the workability and strength properties of geopolymer concrete cured at ambient temperature. Mater Des 2014;62:32–9. https://doi.org/10.1016/J.MATDES.2014.05.001.

[12] Okoye FN, Durgaprasad J, Singh NB. Effect of silica fume on the mechanical properties of fly ash based-geopolymer concrete. Ceram Int 2016;42:3000–6. https://doi.org/10.1016/J.CERAMINT.2015.10.084.

[13] Luhar S, Chaudhary S, Luhar I. Development of rubberized geopolymer concrete: Strength and durability studies. Constr Build Mater 2019;204:740–53. https://doi.org/10.1016/J.CONBUILDMAT.2019.01.185.

[14] Park Y, Abolmaali A, Kim YH, Ghahremannejad M. Compressive strength of fly ash-based geopolymer concrete with crumb rubber partially replacing sand. Constr Build Mater 2016;118:43–51. https://doi.org/10.1016/J.CONBUILDMAT.2016.05.001.

[15] Aly AM, El-Feky MS, Kohail M, Nasr ESAR. Performance of geopolymer concrete containing recycled rubber. Constr Build Mater 2019;207:136–44. https://doi.org/10.1016/J.CONBUILDMAT.2019.02.121.

[16] Albitar M, Mohamed Ali MS, Visintin P, Drechsler M. Effect of granulated lead smelter slag on strength of fly ash-based geopolymer concrete. Constr Build Mater 2015;83:128–35. https://doi.org/10.1016/J.CONBUILDMAT.2015.03.009.

[17] Muttashar HL, Ariffin MAM, Hussein MN, Hussin MW, Ishaq S Bin. Self-compacting geopolymer concrete with spend garnet as sand replacement. J Build Eng 2018;15:85–94. https://doi.org/10.1016/J.JOBE.2017.10.007.

[18] Albidah A, Alghannam M, Abbas H, Almusallam T, Al-Salloum Y. Characteristics of metakaolin-based geopolymer concrete for different mix design parameters. J Mater Res Technol 2021;10:84–98. https://doi.org/10.1016/J.JMRT.2020.11.104.

[19] Pothisiri T, Panedpojaman P. Modeling of bonding between steel rebar and concrete at elevated temperatures. Constr Build Mater 2012;27:130–40. https://doi.org/10.1016/J.CONBUILDMAT.2011.08.014.

[20] Yu R, Spiesz P, Brouwers HJH. Development of an eco-friendly Ultra-High Performance Concrete (UHPC) with efficient cement and mineral admixtures uses. Cem Concr Compos 2015;55:383–94. https://doi.org/10.1016/J.CEMCONCOMP.2014.09.024.

[21] Zanotti C, Borges PHR, Bhutta A, Banthia N. Bond strength between concrete substrate and metakaolin geopolymer repair mortar: Effect of curing regime and PVA fiber reinforcement. Cem Concr Compos 2017;80:307–16. https://doi.org/10.1016/J.CEMCONCOMP.2016.12.014.

[22] Dutta S, Mandal JN. Model Studies on Geocell-Reinforced Fly Ash Bed Overlying Soft Clay. J Mater Civ Eng 2015;28:04015091.

https://doi.org/10.1061/(ASCE)MT.1943-5533.0001356.

[23] Tanyildizi H, Yonar Y. Mechanical properties of geopolymer concrete containing polyvinyl alcohol fiber exposed to high temperature. Constr Build Mater 2016;126:381–7. https://doi.org/10.1016/J.CONBUILDMAT.2016.09.001.

[24] Ganesh AC, Muthukannan M. Development of high performance sustainable optimized fiber reinforced geopolymer concrete and prediction of compressive strength. J Clean Prod 2021;282:124543. https://doi.org/10.1016/J.JCLEPRO.2020.124543.

[25] Vaidya S, Allouche EN. Strain sensing of carbon fiber reinforced geopolymer concrete. Mater Struct Constr 2011;44:1467–75. https://doi.org/10.1617/S11527-011-9711-3/METRICS.

[26] Albidah A, Abadel A, Alrshoudi F, Altheeb A, Abbas H, Al-Salloum Y. Bond strength between concrete substrate and metakaolin geopolymer repair mortars at ambient and elevated temperatures. J Mater Res Technol 2020;9:10732–45. https://doi.org/10.1016/J.JMRT.2020.07.092.

[27] TAHERI AMIRI MJ, Ashrafian A, Haghighi FR, Javaheri Barforooshi M. Prediction of the Compressive Strength of Self-compacting Concrete containing Rice Husk Ash using Data Driven Models. Modares Civ Eng J 2019;19:209–21.

[28] Razeghi HR, Ghadir P, Javadi AA. Mechanical Strength of Saline Sandy Soils Stabilized with Alkali-Activated Cements. Sustain 2022, Vol 14, Page 13669 2022;14:13669. https://doi.org/10.3390/SU142013669.

[29] Ghadir P, Razeghi HR. Effects of sodium chloride on the mechanical strength of alkali activated volcanic ash and slag pastes under room and elevated temperatures. Constr Build Mater 2022;344:128113. https://doi.org/10.1016/J.CONBUILDMAT.2022.128113.

[30] Ashrafian A, Panahi E, Salehi S, Karoglou M, Asteris PG. Mapping the strength of agro-ecological lightweight concrete containing oil palm by-product using artificial intelligence techniques. Structures 2023;48:1209–29. https://doi.org/10.1016/J.ISTRUC.2022.12.108.

[31] Ashrafian A, Shahmansouri AA, Akbarzadeh Bengar H, Behnood A. Post-fire behavior evaluation of concrete mixtures containing natural zeolite using a novel metaheuristic-based machine learning method. Arch Civ Mech Eng 2022;22:101. https://doi.org/10.1007/s43452-022-00415-7.

[32] C618 Standard Specification for Coal Fly Ash and Raw or - Google Scholar n.d.

[33] ASTM C39 / C39M Standard Test Method for Compressive - Google Scholar n.d.

[34] Belalia Douma O, Boukhatem B, Ghrici M, Tagnit-Hamou A. Prediction of properties of self-compacting concrete containing fly ash using artificial neural network. Neural Comput Appl 2017;28:707–18. https://doi.org/10.1007/S00521-016-2368-7/METRICS.

[35] Ashrafian A, Taheri Amiri MJ, haghighi farshidreza. Modeling the Slump Flow of Self-Compacting Concrete Incorporating Metakaolin Using Soft Computing Techniques. J Struct Constr Eng 2019;6:5–20. https://doi.org/10.22065/jsce.2018.90214.1243.

[36] An D, Kim NH, Choi JH. Practical options for selecting data-driven or physics-based prognostics algorithms with reviews. Reliab Eng Syst Saf 2015;133:223–36. https://doi.org/10.1016/J.RESS.2014.09.014.

[37] Rajaee T, Shahabi A. Evaluation of wavelet-GEP and wavelet-ANN hybrid models for prediction of total nitrogen concentration in coastal marine waters. Arab J Geosci 2016;9:1–15. https://doi.org/10.1007/S12517-015-2220-X/METRICS.

[38] Komasi M, Goudarzi H, Behniya A. Studying the process of space-time ground water level by support vector machine and Kriging Method in GIS (case study: silakhor plain). J Water Soil Conserv 2017;24:195–209. https://doi.org/10.22069/JWSC.2017.11640.2611.

[39] Barman M, Choudhury NBD, Sutradhar S. A regional hybrid GOA-SVM model based on similar day approach for short-term load

forecasting in Assam, India. Energy 2018;145:710–20.

[40] Meng E, Huang S, Huang Q, Fang W, Wu L, Wang L. A robust method for non-stationary streamflow prediction based on improved EMD-SVM model. J Hydrol 2019;568:462–78. https://doi.org/10.1016/J.JHYDROL.2018.11.015.

[41] Cortes C, Vapnik V. Support-Vector Networks. Mach Learn 1995;20:273–97. https://doi.org/10.1023/A:1022627411411.

[42] Ashrafian A, Shokri F, Taheri Amiri MJ, Yaseen ZM, Rezaie-Balf M. Compressive strength of Foamed Cellular Lightweight Concrete simulation: New development of hybrid artificial intelligence model. Constr Build Mater 2020;230:117048. https://doi.org/10.1016/J.CONBUILDMAT.2019.117048.

[43] Eskandar H, Sadollah A, Bahreininejad A, Hamdi M. Water cycle algorithm – A novel metaheuristic optimization method for solving constrained engineering optimization problems. Comput Struct 2012;110–111:151–66. https://doi.org/10.1016/J.COMPSTRUC.2012.07.010.

[44] Noparast M, Hematian M, Ashrafian A, Javad M, Amiri T, Azarijafari H. Development of a non-dominated sorting genetic algorithm for implementing circular economy strategies in the concrete industry. Sustain Prod Consum 2021;27:933–46. https://doi.org/10.1016/j.spc.2021.02.009.

[45] Zhang W, Lee D, Lee J, Lee C. Residual strength of concrete subjected to fatigue based on machine learning technique. Struct Concr 2022;23:2274–87. https://doi.org/10.1002/SUCO.202100082.

[46] Asteris PG, Lourenço PB, Hajihassani M, Adami CEN, Lemonis ME, Skentou AD, et al. Soft computing-based models for the prediction of masonry compressive strength. Eng Struct 2021;248:113276. https://doi.org/10.1016/J.ENGSTRUCT.2021.113276.